Accepted Manuscript

Discovery of potent and novel smoothened antagonists *via* structure-based virtual screening and biological assays

Wenfeng Lu, Dihua Zhang, Haikuo Ma, Sheng Tian, Jiyue Zheng, Qin Wang, Lusong Luo, Xiaohu Zhang

PII: S0223-5234(18)30448-3

DOI: 10.1016/j.ejmech.2018.05.035

Reference: EJMECH 10446

To appear in: *European Journal of Medicinal Chemistry*

Received Date: 26 February 2018

Revised Date: 19 May 2018

Accepted Date: 22 May 2018

Please cite this article as: W. Lu, D. Zhang, H. Ma, S. Tian, J. Zheng, Q. Wang, L. Luo, X. Zhang, Discovery of potent and novel smoothened antagonists *via* structure-based virtual screening and biological assays, *European Journal of Medicinal Chemistry* (2018), doi: 10.1016/j.ejmech.2018.05.035.

Discovery of Potent and Novel Smoothened Antagonists *via* Structure-Based Virtual Screening and Biological Assays

Wenfeng Lu[a,1], Dihua Zhang[a,1], Haikuo Ma[a,b,*], Sheng Tian[a,d,*], Jiyue Zheng[a], Qin Wang[c], Lusong Luo[c], and Xiaohu Zhang[a,*]

[a]Jiangsu Key Laboratory of Neuropsychiatric Diseases and College of Pharmaceutical Sciences, Soochow University, Suzhou, Jiangsu 215123, P.R. China

[b]Cyrus Tang Hematology Center, Jiangsu Institute of Hematology and Collaborative Innovation Center of Hematology, Soochow University, Suzhou 215123, P.R. China.

[c]BeiGene (Beijing) Co., Ltd., No. 30 Science Park Road, Zhongguancun Life Science Park, Beijing 102206, P.R. China.

[d]Institute of Functional Nano & Soft Materials (FUNSOM), Soochow University, Suzhou, Jiangsu 215123, P. R. China

[1] these authors contributed equally to this paper

Corresponding Authors：

E-mail: xiaohuzhang@suda.edu.cn; stian@suda.edu.cn; mahaikuo123@163.com

Keywords: smoothened receptor, antagonist, virtual screening, molecular docking

For Table of Contents Use Only

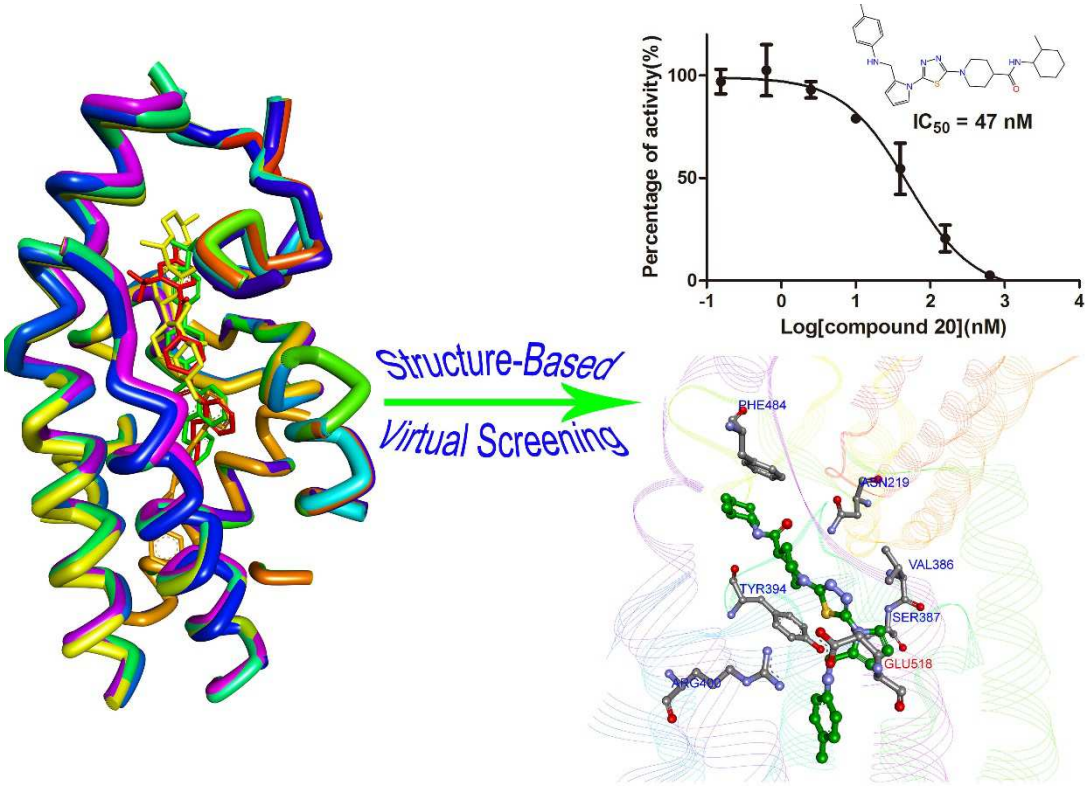

Abstract

The Hedgehog (Hh) signaling pathway plays a critical role in controlling patterning, growth and cell migration during embryonic development. Aberrant activation of Hh signaling has been linked to tumorigenesis in various cancers, such as basal cell carcinoma (BCC) and medulloblastoma. As a key member of the Hh pathway, the Smoothened (Smo) receptor, a member of the G protein-coupled receptor (GPCR) family, has emerged as an attractive therapeutic target for the treatment and prevention of human cancers. The recent determination of several crystal structures of Smo in complex with different antagonists offers the possibility to perform structure-based virtual screening for discovering potent Smo antagonists with distinct chemical scaffolds. In this study, based on the two Smo crystal complexes with the best capacity to distinguish the known Smo antagonists from decoys, the molecular docking-based virtual screening was conducted to identify promising Smo antagonists from ChemDiv library. A total of 21 structurally novel and diverse compounds were selected for experimental testing, and six of them exhibited significant inhibitory activity against the Hh pathway activation (IC_{50} < 10 μM) in a GRE (Gli-responsive element) reporter gene assay. Specifically, the most potent compound (compound **20**: 47 nM) showed comparable Hh signaling inhibition to vismodegib (46 nM). Compound **20** was further confirmed to be a potent Smo antagonist in a fluorescence based competitive binding assay. Optimization using substructure searching method led to the discovery of 12 analogues of compound **20** with decent Hh pathway inhibition activity, including four compounds with IC_{50} lower than 1 μM. The important residues uncovered by binding free energy calculation (MM/GBSA) and binding free energy decomposition were highlighted and discussed. These findings suggest that the novel scaffold afforded by compound **20** can be used as a good starting point for further modification/optimization and the clarified interaction patterns may also guide us to find more potent Smo antagonists.

1. Introduction

The Hedgehog (Hh) signaling cascade plays a critical role in controlling patterning, growth and cell migration during embryonic development and inhibition of the Hh pathway at this stage has been shown to cause cyclopia and other developmental defects.[1-4] In adult organisms, the Hh pathway is down-regulated significantly and contributes to the maintenance and regeneration of certain tissues such as skin and bone. In vertebrates, there are three Hh homologues including Sonic Hedgehog (Shh), Desert Hedgehog (Dhh) and Indian Hedgehog (Ihh). Typically, the Hh signaling can be activated when the Hh ligands bind to their receptor Patched (Ptch) directly, alleviating the inhibition effect of Ptch on Smoothened (Smo), a class F receptor of the G protein-coupled receptor (GPCR) family. The activated Smo then translocate from intracellular to the cell membrane, leading to the activation of Hh signaling transcription factors of the Gli family, which regulates cell proliferation, differentiation and survival. It was reported that deregulation or hyperactivation of the Hh signaling has been linked to tumorigenesis in various cancers, such as basal cell carcinoma (BCC), medulloblastoma, leukemia, rhabdomyosarcoma, lung, breast and prostate cancers.[2, 5-9] Therefore, inhibition of the aberrant Hh signaling has emerged as an attractive approach for the treatment and prevention of human cancers.

The first reported Hh signaling pathway inhibitor was cyclopamine (Figure 1), which was isolated from *Veratrum californicum* because of its teratogenicity in sheep. It was later identified as a Smo antagonist.[10, 11] More efforts were made to develop Smo antagonists and a number of Smo antagonists have entered to advanced clinical trials successfully.[12-15] Encouragingly, vismodegib (GDC-0449, Figure 1)[16, 17] developed by Roche/Genentech was approved by the FDA in January 2012 for the treatment of locally advanced or inoperable metastatic BCC. Moreover, in July 2015, sonidegib (NVP-LDE225, Figure 1)[18] from Novartis also received FDA approval for use in treating locally advanced BCC. These approvals suggest that Smo receptor is an ideal therapeutic target and boosted interest in finding/designing potent and novel Smo antagonists for treating Hh signaling pathway related diseases. In spite of

their therapeutic effectiveness, side effects including diarrhea, muscle spasms, weight loss and tiredness occurred in many patients with the clinical treatment of vismodegib or sonidegib. Moreover, drug resistance due to Smo mutations or downstream ligand-independent pathway activation has also been reported by treating with vismodegib.[19-21] Consequently, there remains ongoing need to explore potent Smo antagonists with novel scaffolds.

In pursuit of potent Smo antagonists with novel chemical scaffolds, several optimization strategies, such as “scaffold hopping”, were proposed by our group and a number of novel chemical scaffolds, including tetrahydroimidazo[1,2-*a*]pyrazine,[22] tetrahydrothiazolo[5,4-*c*]-pyridine,[23] and tetrahydropyrido[4,3-*d*]pyrimidine,[24] with satisfactory binding affinities against the Smo receptor were rationally designed. Other promising Smo antagonists through chemical modifications/optimizations had also been reported in the past few years (Figure 1).[25-31]

As an important complementary approach to high-throughput screening (HTS), virtual screening (VS) has received increasing attentions and been widely used for hit identifications in drug discovery.[32, 33] In 2010, Manetti and co-workers generated and applied a pharmacophore model based on a set of Smo antagonists with known antagonistic activities for carrying out ligand-based virtual screening (LBVS) of commercial libraries. An acylthiourea (MRT-10) was identified and validated as a potent Smo antagonist with binding affinity in the micromolar range (IC_{50} = 0.65 μM).[34] Subsequent optimizations led to the identification of more promising Smo antagonists with increased inhibition potency, MRT-14 (IC_{50} = 0.16 μM)[34] or novel scaffold, MRT-83 (IC_{50} = ~ 0.01 μM).[35, 36] Besides, with the rapid development of structural biology, several 3D crystal structures of Smo in complex with different antagonists were resolved successfully by X-ray diffraction in recent years. It has opened up new avenues for Smo antagonists screening/designing.[37] Based on the precise knowledge and explicit interaction patterns afforded by the available crystal structures of Smo in complex with different antagonists, the structure-based virtual screening (SBVS), especially molecular docking-based VS, can be employed to obtain potent Smo antagonists. In 2016, based on the crystal complex of the Smo

receptor (PDB ID: 4JKV), Lacroix et al. identified four novel Smo antagonists with IC_{50} values better than 50 μM from the clean lead-like library of ZINC through DOCK3.6-based virtual screening. One of the most active Smo antagonists was resilient to the resistance-conferring mutation D473H, from which vismodegib suffered in patients.[38] Besides, it should be noted that the predictions from molecular docking based on the different complexes for the same target may differ greatly because the binding patterns characterized by these different complexes are varied in the previous studies.[39-45] Comparing the prediction capacities of docking-based VS by applying different crystal complexes in molecular docking and selecting the most reliable complexes to screen commercial libraries seems to be a more reasonable way to identify promising active compounds for a specified target.

To our knowledge, this is the first case to evaluate the prediction capacity of docking-based virtual screening comprehensively for discovering promising Smo antagonists. Based on four available Smo crystal complexes, the performances of *Glide* docking-based VS were compared using two well-prepared validation datasets (VD1 and VD2). Two Smo crystal complexes with the best discrimination power were verified as most reliable docking structures and used to screen the ChemDiv library. Following by drug-likeness and ADME/T predictions, REOS filtering and structural clustering, 21 compounds were selected and purchased for experimental testing. Six compounds exhibited significant inhibitory activity against Hh pathway activation (IC_{50} < 10 μM) and the most potent hit (compound **20**: 47 nM) showed comparable inhibitory activity to the positive control compound (vismodegib: 46 nM) in a GRE (Gli-responsive element) reporter gene assay. Compound **20** was further confirmed to be a potent Smo antagonist in a fluorescence based competitive binding assay. Then, based on the scaffold architecture of compound **20**, the substructure searching method was employed to find more promising antagonists of Smo receptor and 12 analogues of compound **20** were chosen and synthesized for biological testing. All analogues showed quite acceptable antagonistic activity of Smo receptor (IC_{50} < 10 μM) including four most potent analogues with IC_{50} below 1 μM. Subsequently, the Molecular Mechanics/Generalized Born Surface Area (MM/GBSA) binding free

energy calculation and binding free energy decomposition were applied to detect the differences of antagonistic activity against the Smo receptor for compound **20** and 12 analogues. The favorable and unfavorable residues for ligand binding were clearly uncovered and the structure-activity relationships (SARs) of 12 analogues of compound **20** were also discussed.

2. Results and Discussion

2.1. Docking-based virtual screening pipeline

Prior to virtual screening campaign, the performances of molecular docking of four Smo crystal complexes were evaluated and compared by using SP and XP scoring modes of *Glide*. Firstly, the "docking power", which is an important index of docking reliability for reproducing the experimental binding mode/conformation of co-crystallized ligand was examined. For each Smo crystal complex, the native antagonist was extracted from the crystal complex and re-docked into the respective binding site/pocket. The root-mean-squared-deviation (RMSD) between the docking pose and experimental conformation was calculated. Generally speaking, reliable molecular docking can be achieved when the RMSD $\leq$ 2.0 Å. As shown in Table 1, the Smo crystal complex (PDB ID: 4N4W) can satisfy the requirement of RMSD and the RMSD values of co-crystallized antagonists for the remaining Smo crystal complexes were slight higher than 2.0 Å by using SP or XP scoring functions of *Glide*. We aligned the co-crystallized antagonist with the predicted binding conformations using the SP and XP scoring modes of *Glide* for 4JKV and 4QIM. The results demonstrated that the near native co-crystallized antagonists and the most important interaction patterns of the two Smo crystal complexes could be well reproduced by *Glide* (Figure S1 in the Supporting Information). Then, compared with "docking power", the "discrimination power" of molecular docking, which is the capacity of distinguishing the known antagonists from presumed non-antagonists of Smo is a more practical index used in docking-based VS campaign. The significance of the difference between the means of docking score distributions of known antagonists and

non-antagonists in VD1 and VD2 was assessed by applying student's *t* test. For VD1 (Table 1 and Figure 2), the known antagonists and non-antagonists of Smo can be well distinguished from each other, indicating by quite lower *P*-values ($< 10^{-50}$) using SP or XP modes of *Glide*. The most reliable "discrimination power" can be obtained by using SP scoring function based on the 4QIM crystal structure (*P*-values = 0). Similarly, the *Glide* docking can also achieve reliable prediction capacity for VD2 in terms of the *P*-values (Table 1 and Figure 3). By applying 4JKV as the docking complex, the most reliable "discrimination power" can be achieved ($P = 2.21\times10^{-162}$) by using SP mode of *Glide*.

According to the performances of docking-based VS based on four Smo crystal complexes, 4JKV and 4QIM were chosen in the following VS campaign. The scoring functions including high-throughput virtual screening (HTVS), SP and XP of *Glide* docking were employed to carry out the sequential VS strategy. Briefly, the 100000 top-ranked compounds of the prepared ChemDiv library scored by HTVS were saved and set to *Glide* docking by using SP mode. Then, the 5000 top-ranked compounds obtained by using SP scoring function were re-docked and scored using the XP mode. Finally, 1000 top-ranked compounds for each Smo crystal complex were retained for the following analysis. By removing duplicates, the remaining compounds from docking-based VS against 4JKV and 4QIM were evaluated by "Rule-of Five" proposed by Lipinski[46] and drug-likeness models developed in our group.[47, 48] The molecules with toxic, reactive, or undesirable functional groups were also removed by applying rapid elimination of swill (REOS).[49] Then, by filtering the compounds with more than two chiral centers, the remaining compounds were structural clustered based on the similarity index (*Tanimoto coefficient*) calculated using *MACCS* structural keys. By setting the cutoff value of *Tanimoto coefficient* to 0.7, the compounds with the lowest docking scores were selected in each cluster. Finally, 21 compounds were chosen and purchased from ChemDiv database for biological testing.

2.2. *In vitro* biological activity of virtual screening compounds

To evaluate the Hh signaling inhibition activity of the 21 candidate compounds predicted by the docking-based VS based on two Smo crystal complexes (4JKV and 4QIM), we used NIH3T3-GRE-Luc reporter gene assay as described in the experimental protocols section as a screening assay. The results were summarized in Table 2, we found that 6 compounds (**14**, **15**, **17**, **18**, **19** and **20**) exhibited decent Hh signaling pathway inhibitory activity, with $IC_{50} < 10\ \mu M$. Among them, compound **14** exhibited good inhibitory activity at 950 nM, while compound **20** demonstrated excellent Hh inhibition activity at $IC_{50} = 47$ nM (Figure 4). The IC_{50} curves for other five compounds (**14**, **15**, **17**, **18** and **19**) were depicted in Figure S2 in the Supporting Information. As a hit from VS, compound **20** was remarkably equally potent at inhibiting Hh signaling compared with the marketed drug vismodegib (compound **22**, $IC_{50} = 46$ nM). As a precaution, we synthesized compound **20** in our laboratory and tested the synthetic compound in the same screening assay. The results were the same as the commercial compound, thus validating the results of the VS hit. The compound **20** was further confirmed to be a potent Smo antagonist in the fluorescence based BODIPY-Cyclopamine competitive binding assay as described in the experimental protocols section and vismodegib was used as a reference (Figure 5).

The structures for the 6 ligands of the Smo receptor ($IC_{50} < 10\ \mu M$) from the VS are shown in Figure 6 and the remaining studied compounds can be found in Figure S3 in the Supporting Information. Then, the structures of 6 identified Smo ligands were compared with the known antagonists of Smo receptor from Binding DB[50] by using default setting of *Find Similar Molecules by Fingerprints* mode in DS3.1.[51] The results illustrated that the 6 identified Smo ligands did not share high similarity with any known Smo antagonists (Table 2). For the two most potent Smo ligands, compounds **14** and **20**, the pairwise similarities (*Tanimoto coefficient*) were only 0.36 and 0.29, respectively. In addition, it should be noted that the two most potent Smo ligands were obtained by applying different Smo crystal complexes in *Glide* docking (compound **14** from 4QIM and compound **20** from 4JKV), indicating that evaluating and comparing the prediction capacity of different crystal structures prior to VS pipeline is quite necessary. The schematic representation of the predicted interaction

patterns derived from *Glide* docking between the Smo and compounds **14** and **20** are depicted in Figure 7.

2.3. Hit confirmation and Structural-Activity-Relationship discussions.

Based on the scaffold architecture (Murcko framework) of the most potent Smo antagonist (compound **20**) identified from docking-based VS, substructure searching was applied to screen the whole ChemDiv library. The pairwise similarities (*Tanimoto coefficient*) between compound **20** and each compound in the ChemDiv library were calculated based on the *MACCS Structural Keys* (Bit packed) fingerprints in MOE. The pairwise similarities over 85% were saved. Then, according to knowledge-based experiences, 12 representative analogues of compound **20** were selected and synthesized for ultimately experimental testing. As can be seen from Table 3, all analogues showed quite acceptable inhibitory activity (IC_{50} < 10 μM) against Hh pathway signaling and four of them with IC_{50} below 1 μM. Nevertheless, the most potent analogue (compound **20-2**: 58 nM) showed no improved binding affinity compared with the parent compound (compound **20**). Then, for detecting the differences of antagonistic activities of compound **20** and 12 analogues, all compounds were docked into the binding pocket of the best Smo crystal complex (PDB ID: 4JKV) using SP scoring function of *Glide* docking. As shown in Figure 8a, the correlation coefficient (r^2) between the experimental pIC_{50} and the docking scores was only 0.346. The results demonstrated that the predicted docking scores have poor capacity for ranking the actual experimental antagonistic activity. Thus, the binding free energy calculation and binding free energy decomposition were utilized to analyze the interaction patterns between the studied compounds and Smo receptor. The predicted conformations for compound **20** and 12 analogues interacting with Smo receptor (PDB ID: 4JKV) from *Glide* docking were optimized and rescored by using the MM/GBSA approach. The detailed protocols for the molecular dynamics (MD) simulation and MM/GBSA binding free energy calculations/decompositions was described in the Supporting Information. Obviously, the correlation coefficient between the antagonistic activities and the binding free energies calculated by the

MM/GBSA can achieved quite satisfied prediction accuracy (r^2 = 0.733) (Figure 8b). Compared with the *Glide* docking, the MM/GBSA rescoring has better capability to rank the bioactivities for this series of analogues represented by compound **20**.

In order to reveal the key residues for Smo antagonist binding, the total binding free energies predicted by the MM/GBSA (ε_{in} = 1) of compound **20** and three representative analogues (compounds **20-3**, **20-5** and **20-12**) were decomposed quantitatively into individual residue contributions.[52-54] The identified key residues (favorable or unfavorable for ligand binding) and the comparison of the antagonist-residues spectra of four compounds were depicted in Figure 9. As shown in Figure 9a, the most favorable residues for compound **20** interacting with Smo receptor were Asn219, Val386, Ser387, Tyr394, Arg400 and Phe484, and their contributions to predicted total binding free energies (ΔG_{pred}) are all lower than -2.0 kcal/mol. Meanwhile, the residue Glu518 takes the vast majority of the negative contributions for the compound **20** binding (2.88 kcal/mol). Similar phenomenon can also be observed for compounds **20-3**, **20-5** and **20-12**. Next, in order to understand the effects of different substituents on the antagonistic activity of Smo receptor, the antagonist-residues spectra of four investigated compounds were compared. By replacing 2-methylcyclohexan-1-amine with ethylamine in the R_3 position, the antagonistic activity of compound **20-3** (IC_{50} = 5200 nM) was about 100 times lower than compound **20** (IC_{50} = 47 nM). According to Figures 9b and 9c, we found that the compound **20** and **20-3** share quite similar interactions with Smo receptor. The most significant differences are mainly caused by the interactions with residues Asn219 and Phe484. The energy contributions of Asn219 and Phe484 for compound **20** were -2.90 and -2.55 kcal/mol, and those for compound **20-3** were only -2.20 and -1.77 kcal/mol, respectively. Subsequently, the replacements of 2-methylcyclohexan-1-amine by cyclopropylamine (**20-5**) and pyrrolidin-3-ol (**20-12**) at R_3 group of compound **20** decrease the binding affinity significantly. As shown in the antagonist-residues interaction spectra (Figures 9b, 9d and 9e), the energy contributions of Asn219 for compounds **20-5** and **20-12** were only -0.96 and –0.67 kcal/mol, playing a dominating role in the antagonistic activity difference. Based on these observations, keeping

stable and strong interactions with uncovered favorable residues (Asn219, Val386, Ser387, Tyr394, Arg400 and Phe484) and avoiding the unfavorable interactions primary caused by residue Glu518 are the requirements of Smo antagonists for improving binding affinities. This finding will guide rational-design of more potent antagonists of Smo receptor.

3. Conclusions

In summary, we evaluated and compared the prediction capacities of four available Smo crystal complexes in *Glide* docking-based VS for consideration of the inherent protein flexibility of GPCR targets. Two Smo crystal complexes with the best discrimination power were selected to screen the ChemDiv database. 21 potential hits with novel scaffold were submitted to biological activity testing, and six of them revealed significant inhibitory activity towards Hh signaling pathway activation, including two compounds with IC_{50} values below 1 μM (compound **14**: 950 nM and compound **20**: 47 nM). The compound **20** was further confirmed to be a potent Smo antagonist in a fluorescence based competitive binding assay. The VS strategy presented here may be applied in the drug discovery for targets of interest, especially for GPCR targets. The novel scaffold afforded by compound **20** can also be used as a good starting point for developing promising Smo antagonists.

4. Virtual Screening Pipeline

4.1. Preparation of crystal complexes and validation datasets for docking-based VS

Only five Smo crystal complexes, including 4JKV,[55] 4N4W,[56] 4O9R,[57] 4QIM[56] and 4QIN,[56] have been crystallized and released. The crystal structures of Smo in complex with different antagonists were retrieved from the RCSB Protein Data Bank (PDB).[58] Recently, more Smo crystal complexes were reported with the technology development of structural biology.[59, 60] 4QIN is the crystal complex of an agonist, SAG1.5, interacting with Smo and thus not considered in this work. The

aligned structures and detailed interaction patterns of four Smo crystal complexes were depicted in Figure 10. For each Smo complex, the docking-based VS was carried out using *Glide* in Schrodinger 9.0.[61] The *Protein Preparation Wizard* module of Schrodinger 9.0 was utilized to remove all crystallographic water molecules, add missing side chains and hydrogen atoms, assign protonation states and partial charges with the OPLS2005 force field, and then the minimize procedure of the whole Smo crystal complex terminated until the RMSD of the non-hydrogen atoms reached a maximum default value of 0.3 Å.

Similar to our previous reported study,[51] two independent validation datasets were well-prepared and applied to evaluate the actual prediction capacity of the *Glide* docking-based VS of four Smo crystal complexes. The known antagonists of Smo were retrieved from the BindingDB database.[50] The known antagonists with weak biological binding affinities (IC_{50} or K_i > 2 μM) were removed. Considering the accuracy and efficiency of VS campaign, 300 diverse known antagonists of Smo were randomly chosen based on the 2D similarity (*Tanimoto Coefficient*) of the FCFP_6 fingerprints by using the *Find Diverse Molecules* module in Discovery Studio 3.1.[62] As reported by Kruger and co-workers, it is an effective way to represent the compound space of a decoy set by using commercial database, especially for the VS database is the source of decoy set.[63] Thus, based on the 2D similarity of the FCFP_6 fingerprints, the presumed non-antagonists of the validation dataset 1 (VD1) were selected randomly from the ChemDiv database using the *Find Diverse Molecules* module in Discovery Studio 3.1.[51] To mimic the unbalanced nature of the known antagonists *versus* the non-antagonists of Smo, the ratio of non-antagonists *versus* antagonists was set to 100 in VD1. Then, the validation dataset 2 (VD2), which conforms the rules defined by Cereto-Massague et al., was generated directly by using DecoyFinder 1.1.[64] For each selected Smo antagonist, 36 decoys were chosen from the ChemDiv database ensuring the similarity of five physical descriptors (molecular weight, number of rotatable bonds, total hydrogen bond donors/acceptors and the octanol-water partition coefficient (log*P*) but structural dissimilarity evaluated by *MACCS* fingerprints (*Tanimoto coefficient* < 0.75). Finally, the VD1 with 300 known

antagonists and 30000 non-antagonists and VD2 with 300 known antagonists and 10800 decoys were prepared for the following analysis.

4.2. Molecular docking-based VS procedure

The docking-based VS were carried out by using *Glide* of Schrodinger 9.0.[51] For the four Smo crystal complexes, the performances of docking-based VS were investigated systematically. Firstly, all compounds including known Smo antagonists and decoys in VD1 and VD2 were processed by using the *LigPrep* module in Schrodinger 9.0. The ionized states and tautomers/stereoisomers were generated using *Epik* at pH = 7.0 ± 2.0. For the known antagonists from BindingDB with 3D structural information, the original chiralities were reserved. Considering only 2D structural information available for the decoys selected from the ChemDiv database, different combinations of chiralities were generated, and the maximum number of stereoisomers for each decoy was set to 32. Finally, the number of prepared Smo antagonists was 300, and the numbers of prepared decoys for VD1 and VD2 were 53408 and 22455, respectively.

Then, by applying the *Receptor Grid Generation* component of *Glide* in Schrodinger 9.0, the binding pocket with the size of 10 Å × 10 Å × 10 Å was detected and centered on the mass center of the co-crystallized antagonist for each Smo crystal complex. The other parameters in grid generation were kept as default setting. All compounds of VD1 and VD2 were docked into the four Smo crystal complexes and scored by using two scoring functions (SP: Standard Precision and XP: Extra Precision) embedded in *Glide*. During the initial phase of the *Glide* docking calculation, 5000 poses per compound were generated. Then, the best 400 poses were selected for the following energy minimization using 100 steps of conjugate-gradient minimization process with a dielectric constant of 2.0. Finally, the performances of the *Glide* docking-based VS based on SP and XP modes of four Smo crystal complexes were evaluated and compared.

The ChemDiv database comprising more than 1 million compounds was used as the screening library and all compounds in the ChemDiv database were also

preprocessed by using the *LigPrep* mode in *Glide*. The ionized states and tautomers were generated at pH = 7.0 ± 2.0 by using *Epik*. Then, the different combinations of chiralities were generated and the maximum number of stereoisomers for each compound was set to 32. The prepared ChemDiv library including more than 2.65 million chemical structures was submitted to the docking-based VS campaign.

4.3. Substructure searching

In order to get more promising antagonists of Smo receptor, the substructure searching method in Molecular Operating Environment (MOE)[65] was utilized to find the analogues sharing the similar scaffold architecture (Murcko framework)[66] of the most potent Smo antagonist identified from *Glide* docking-based VS. For compound **20**, 12 representative analogues with different functional groups substitution were selected and synthesized for biological testing.

5. Experimental protocols

5.1. Synthesis procedure of the targeted compound 20 to 20-12

The synthesis and characterization of the intermediates and final compounds can be found in the Supporting Information.

5.2. NIH3T3-GRE-Luc reporter gene assay

The detailed experimental procedures had been reported before.[23, 24] Briefly, NIH3T3 cells (CRL-1658, ATCC) were maintained in DMEM (Gibico) supplemented with 10% FBS (Hyclone). GRE-Luc plasmid was generated by inserting 8x Gli-1 responsive element (GRE) into the multiple cloning site of pGL4.26 vector (Promega). NIH3T3-GRE-Luc reporter cell line was established by hygromycin (Invitrogen) selection after transfected with GRE-Luc luciferase reporter plasmid. Single clones were validated by the induction of luciferase by recombinant sonic hedgehog (sHh) protein or small molecule agonist SAG (ABIN629346). Selected clone was used to monitor the Hh signaling.

The NIH3T3-GRE-Luc cells were maintained in complete culture medium (DMEM with 4 mM L-Gln, 1.5 g/L sodium bicarbonate and 4.5 g/L glucose supplemented with 100 μg/mL hygromycin and 10% FBS). When confluent, the cells were trypsinized and re-suspended in assay medium (0.5% serum-containing DMEM). After 100 μL/well of cells suspension was added to the 96-well-plate (Final cell concentration is 15,000 cells/well), cells were cultured for additional 48 hours before adding the compounds.

Compounds were serially diluted in DMSO and further diluted with assay medium. In an embodiment, 10 nM SAG was added in assay medium as the agonist of Hh signaling. After the compounds and agonist were prepared, the medium was removed carefully. 100 μL of assay medium containing compound and agonist was added to the cell with care. Cell plates were incubated at 37 °C for additional 48 hours. Following the 48 hours incubation, 40 μL /well of luciferase media (Brigh-Glo, Promega) was added to the cells. The plate was incubated at room temperature for 5 minutes under gentle shaking. Luminescence signal was measured with plate reader (PHERAstar FS, BMG). The IC_{50} of compounds was calculated based on the inhibition of luminescence signaling.

5.3. Fluorescence based BODIPY-Cyclopamine competitive binding assay

The detailed experimental procedures had been reported before.[23, 24] Briefly, U2OS-Smo stable clones were established by puromycin (1 μg/mL, Invitrogen) selection after transfection with human Smo-HA-pLVX. Plasmid U2OS-Smo cells were maintained in complete culture medium (DMEM with 4 mM L-Gln, 1.5 g/L sodium bicarbonate and 4.5 g/L glucose supplemented with 100 ng/mL puromycin and 10% FBS). The expression of human Smo was validated with western blot and cell immunofluorescence. BODIPY-Cyclopamine was purchased from Toronto Research Chemicals and dissolved in methanol.

U2OS-Smo cells were plated in 96-well-plate (#3340, Corning), the final cell concentration is 10,000 cells/well in 100 μL 10% serum-containing DMEM. The plates were incubated in 37 °C for additional 48 hours.

U2OS-Smo cells were fixed with 4% paraformaldehyde (PFA) for 20 minutes at room temperature. After removing the PFA buffer, the cells were incubated with DAPI (5 μg/mL) for 10 minutes, followed by twice wash with PBS. After wash, cells were incubated for 2 h at room temperature in PBS containing 100 nM BODIPY-cyclopamine and serial diluted compounds for competitive binding. After incubation, the cells were washed for 3 times with the PBST (PBS buffer supplied with 0.05% Tween-20). The fluorescence images were automatically captured and analyzed by a high content fluorescence imaging system (Arrayscan VTI, Thermo). GDC-0449 was used as reference compound to normalize the data. IC_{50} values were calculated with GraphPad Prism software using the sigmoidal dose-response function. The K_i was calculated following the Cheng-Prusoff equation, as $K_i = IC_{50}/[1 + [\text{BODIPY-cyclopamine}]/K_d)]$. The K_d of BODIPY-cyclopamine for WT-Smo is 255 $\pm$ 57 nM in our experiments.

Supporting Information

1. Figure S1. (a) The aligned structure of the co-crystallized antagonist with the predicted binding conformations using the SP and XP scoring modes of *Glide* for 4JKV; The interaction patterns of (b) crystal structure, (c) the predicted complex using the SP scoring and (d) the predicted complex using the XP scoring for 4JKV.

1. Figure S2. The IC_{50} curves of five promising compounds (**14**, **15**, **17**, **18** and **19**) with decent Hh signaling pathway inhibitory activity ($IC_{50} < 10$ μM).

2. Figure S3. The structures of 15 identified VS hits with IC_{50} above 10 μM of Smo receptor.

3. The detailed protocols for the molecular dynamics (MD) simulation and MM/GBSA binding free energy calculations/decompositions.

4. Synthesis and characterization data.

Author Information

Corresponding Authors

*X. Z. E-mail: xiaohuzhang@suda.edu.cn.
*S. T. E-mail: stian@suda.edu.cn
*H. M. E-mail: mahaikuo123@163.com.

ORCID

Xiaohu Zhang: 0000-0002-0579-1636

Author Contributions

[1]W. L. and D. Z. contributed equally to this paper.

Notes

The authors declare no competing financial interest.

Acknowledgements

This study was supported by the National Natural Science Foundation of China (81473090, 81773561, and 81502982), China Postdoctoral Science Foundation (2016M601884), the Priority Academic Program Development of the Jiangsu Higher Education Institutes (PAPD) and the Jiangsu Key Laboratory of Translational Research for Neuropsychiatric Diseases (BM2013003), Natural Science Foundation of Jiangsu Province (BK20140313).

References:

[1] S. Peukert, K. Miller-Moslin, Small-Molecule Inhibitors of the Hedgehog Signaling Pathway as Cancer Therapeutics, ChemMedChem, 5 (2010) 500-512.
[2] J.M.Y. Ng, T. Curran, The Hedgehog's tale: developing strategies for targeting cancer, Nat. Rev. Cancer, 11 (2011) 493-501.
[3] C. Chiang, L.T.T. Ying, E. Lee, K.E. Young, J.L. Corden, H. Westphal, P.A. Beachy, Cyclopia and defective axial patterning in mice lacking Sonic hedgehog gene function, Nature, 383 (1996) 407-413.
[4] J. Taipale, J.K. Chen, M.K. Cooper, B.L. Wang, R.K. Mann, L. Milenkovic, M.P. Scott, P.A. Beachy, Effects of oncogenic mutations in Smoothened and Patched can be reversed by cyclopamine, Nature, 406 (2000) 1005-1009.
[5] A. Zibat, E. Missiaglia, A. Rosenberger, K. Pritchard-Jones, J. Shipley, H. Hahn, S. Fulda, Activation of the hedgehog pathway confers a poor prognosis in embryonal and fusion gene-negative alveolar rhabdomyosarcoma, Oncogene, 29 (2010) 6323-6330.
[6] L.L. Rubin, F.J. de Sauvage, Targeting the Hedgehog pathway in cancer, Nat. Rev. Drug Discov., 5 (2006) 1026-1033.
[7] P.W. Ingham, The patched gene in development and cancer, Curr. Opin. Genet. Dev., 8 (1998) 88-94.

[8] J.W. Xie, M. Murone, S.M. Luoh, A. Ryan, Q.M. Gu, C.H. Zhang, J.M. Bonifas, C.W. Lam, M. Hynes, A. Goddard, A. Rosenthal, E.H. Epstein, F.J. de Sauvage, Activating Smoothened mutations in sporadic basal-cell carcinoma, Nature, 391 (1998) 90-92.

[9] L. Yang, G. Xie, Q. Fan, J. Xie, Activation of the hedgehog-signaling pathway in human cancer and the clinical implications, Oncogene, 29 (2010) 469-481.

[10] M.K. Cooper, J.A. Porter, K.E. Young, P.A. Beachy, Teratogen-mediated inhibition of target tissue response to Shh signaling, Science, 280 (1998) 1603-1607.

[11] J.K. Chen, J. Taipale, M.K. Cooper, P.A. Beachy, Inhibition of Hedgehog signaling by direct binding of cyclopamine to Smoothened, Genes Dev., 16 (2002) 2743-2748.

[12] M. Ruat, L. Hoch, H. Faure, D. Rognan, Targeting of Smoothened for therapeutic gain, Trends Pharmacol. Sci., 35 (2014) 237-246.

[13] Y. Li, M.i.Y. Maitah, A. Ahmad, D. Kong, B. Bao, F.H. Sarkar, Targeting the Hedgehog signaling pathway for cancer therapy, Expert Opin. Ther. Targets, 16 (2012) 49-66.

[14] N. Mahindroo, C. Punchihewa, N. Fujii, Hedgehog-Gli Signaling Pathway Inhibitors as Anticancer Agents, J. Med. Chem., 52 (2009) 3829-3845.

[15] T.N. Trinh, E.A. McLaughlin, C.P. Gordon, A. McCluskey, Hedgehog signalling pathway inhibitors as cancer suppressing agents, MedChemComm, 5 (2014) 117-133.

[16] K.D. Robarge, S.A. Brunton, G.M. Castanedo, Y. Cui, M.S. Dina, R. Goldsmith, S.E. Gould, O. Guichert, J.L. Gunzner, J. Halladay, W. Jia, C. Khojasteh, M.F.T. Koehler, K. Kotkow, H. La, R.L. LaLonde, K. Lau, L. Lee, D. Marshall, J.C. Marsters, Jr., L.J. Murray, C. Qian, L.L. Rubin, L. Salphati, M.S. Stanley, J.H.A. Stibbard, D.P. Sutherlin, S. Ubhayaker, S. Wang, S. Wong, M. Xie, GDC-0449-A potent inhibitor of the hedgehog pathway, Bioorg. Med. Chem. Lett., 19 (2009) 5576-5581.

[17] S.E. Gould, J.A. Low, J.C. Marsters, Jr., K. Robarge, L.L. Rubin, F.J. de Sauvage, D.P. Sutherlin, H. Wong, R.L. Yauch, Discovery and preclinical development of vismodegib, Expert Opin. Drug Discov., 9 (2014) 969-984.

[18] S. Pan, X. Wu, J. Jiang, W. Gao, Y. Wan, D. Cheng, D. Han, J. Liu, N.P. Englund, Y. Wang, S. Peukert, K. Miller-Moslin, J. Yuan, R. Guo, M. Matsumoto, A. Vattay, Y. Jiang, J. Tsao, F. Sun, A.C. Pferdekamper, S. Dodd, T. Tuntland, W. Maniara, J.F. Kelleher, III, Y.-m. Yao, M. Warmuth, J. Williams, M. Dorsch, Discovery of NVP-LDE225, a Potent and Selective Smoothened Antagonist, ACS Med. Chem. Lett., 1 (2010) 130-134.

[19] G.J.P. Dijkgraaf, B. Alicke, L. Weinmann, T. Januario, K. West, Z. Modrusan, D. Burdick, R. Goldsmith, K. Robarge, D. Sutherlin, S.J. Scales, S.E. Gould, R.L. Yauch, F.J. de Sauvage, Small Molecule Inhibition of GDC-0449 Refractory Smoothened Mutants and Downstream Mechanisms of Drug Resistance, Cancer Res., 71 (2011) 435-444.

[20] S.X. Atwood, K.Y. Sarin, R.J. Whitson, J.R. Li, G. Kim, M. Rezaee, M.S. Ally, J. Kim, C. Yao, A.L.S. Chang, A.E. Oro, J.Y. Tang, Smoothened Variants Explain the Majority of Drug Resistance in Basal Cell Carcinoma, Cancer Cell, 27 (2015) 342-353.

[21] R.L. Yauch, G.J.P. Dijkgraaf, B. Alicke, T. Januario, C.P. Ahn, T. Holcomb, K. Pujara, J. Stinson, C.A. Callahan, T. Tang, J.F. Bazan, Z. Kan, S. Seshagiri, C.L. Hann, S.E. Gould, J.A. Low, C.M. Rudin, F.J. de Sauvage, Smoothened Mutation Confers Resistance to a Hedgehog Pathway Inhibitor in Medulloblastoma, Science, 326 (2009) 572-574.

[22] W. Lu, D. Geng, Z. Sun, Z. Yang, H. Ma, J. Zheng, X. Zhang, Scaffold hopping approach to a new series of smoothened antagonists, Bioorg. Med. Chem. Lett., 24 (2014) 2300-2304.

[23] H. Ma, W. Lu, Z. Sun, L. Luo, D. Geng, Z. Yang, E. Li, J. Zheng, M. Wang, H. Zhang, S. Yang, X.

Zhang, Design, synthesis, and structure-activity-relationship of tetrahydrothiazolopyridine derivatives as potent smoothened antagonists, Eur. J. Med. Chem., 89 (2015) 721-732.

[24] W. Lu, Y. Liu, H. Ma, J. Zheng, S. Tian, Z. Sun, L. Luo, J. Li, H. Zhang, Z.-J. Yang, X. Zhang, Design, Synthesis, and Structure-Activity Relationship of Tetrahydropyrido 4,3-d pyrimidine Derivatives as Potent Smoothened Antagonists with in Vivo Activity, ACS Chem. Neurosci., 8 (2017) 1980-1994.

[25] E. Muraglia, J.M. Ontoria, D. Branca, G. Dessole, A. Bresciani, M. Fonsi, C. Giuliano, L.L. Bufi, E. Monteagudo, M.C. Palumbi, C. Torrisi, M. Rowley, C. Steinkuehler, P. Jones, N-(2-alkylaminoethyl)-4-(1,2,4-oxadiazol-5-yl)piperazine-1-carboxamides as highly potent smoothened antagonists, Bioorg. Med. Chem. Lett., 21 (2011) 5283-5288.

[26] S. Peukert, F. He, M. Dai, R. Zhang, Y. Sun, K. Miller-Moslin, M. McEwan, B. Lagu, K. Wang, N. Yusuff, A. Bourret, A. Ramamurthy, W. Maniara, A. Amaral, A. Vattay, A. Wang, R. Guo, J. Yuan, J. Green, J. Williams, S. Buonamici, J.F. Kelleher, III, M. Dorsch, Discovery of NVP-LEQ506, a Second-Generation Inhibitor of Smoothened, ChemMedChem, 8 (2013) 1261-1265.

[27] G. Liu, D. Xue, J. Yang, J. Wan, X. Liu, W. Huang, J. Li, Y.-Q. Long, W. Tan, A. Zhang, Design, Synthesis, and Pharmacological Evaluation of 2-(2,5-Dimethyl-5,6,7,8-tetrahydroquinolin-8-yl)-N-aryl Propanamides as Novel Smoothened (Smo) Antagonists, J. Med. Chem., 59 (2016) 11050-11068.

[28] R. Alfonsi, B. Botta, S. Cacchi, L. Di Marcotullio, G. Fabrizi, R. Faedda, A. Goggiamani, A. Iazzetti, M. Mori, Design, Palladium-Catalyzed Synthesis, and Biological Investigation of 2-Substituted 3-Aroylquinolin-4(1H)-ones as Inhibitors of the Hedgehog Signaling Pathway, J. Med. Chem., 60 (2017) 1469-1477.

[29] Z. Peng, J.W. Wong, E.C. Hansen, A.L.A. Puchlopek-Dermenci, H.J. Clarke, Development of a Concise, Asymmetric Synthesis of a Smoothened Receptor (SMO) inhibitor: Enzymatic Transamination of a 4-Piperidinone with Dynamic Kinetic Resolution, Org. Lett., 16 (2014) 860-863.

[30] T.-M. Wu, D.-C. Wang, P. Xiang, J.-N. Zhang, Y.-X. Sang, H.-J. Lin, J. Chen, G. Xie, H. Song, Y.-L. Zhao, Y.-M. Xie, Synthesis and biological evaluation of novel benzamide derivatives as potent smoothened antagonists, Bioorg. Med. Chem. Lett., 24 (2014) 1426-1431.

[31] J. Wang, R.A. Mook, Jr., J. Lu, D.M. Gooden, A. Ribeiro, A. Guo, L.S. Barak, H.K. Lyerly, W. Chen, Identification of a novel Smoothened antagonist that potently suppresses Hedgehog signaling, Bioorg. Med. Chem., 20 (2012) 6751-6757.

[32] F. Bajorath, Integration of virtual and high-throughput screening, Nat. Rev. Drug Discov., 1 (2002) 882-894.

[33] T.J. Hou, X.J. Xu, Recent development and application of virtual screening in drug discovery: An overview, Curr. Pharm. Des., 10 (2004) 1011-1033.

[34] F. Manetti, H. Faure, H. Roudaut, T. Gorojankina, E. Traiffort, A. Schoenfelder, A. Mann, A. Solinas, M. Taddei, M. Ruat, Virtual Screening-Based Discovery and Mechanistic Characterization of the Acylthiourea MRT-10 Family as Smoothened Antagonists, Mol. Pharmacol., 78 (2010) 658-665.

[35] H. Roudaut, E. Traiffort, T. Gorojankina, L. Vincent, H. Faure, A. Schoenfelder, A. Mann, F. Manetti, A. Solinas, M. Taddei, M. Ruat, Identification and Mechanism of Action of the Acylguanidine MRT-83, a Novel Potent Smoothened Antagonist, Mol. Pharmacol., 79 (2011) 453-460.

[36] A. Solinas, H. Faure, H. Roudaut, E. Traiffort, A. Schoenfede, A. Mann, F. Manetti, M. Taddei, M. Ruat, Acylthiourea, Acylurea, and Acylguanidine Derivatives with Potent Hedgehog Inhibiting Activity, J. Med. Chem., 55 (2012) 1559-1571.

[37] R.M. Cooke, A.J.H. Brown, F.H. Marshall, J.S. Mason, Structures of G protein-coupled receptors

reveal new opportunities for drug discovery, Drug Discov. Today, 20 (2015) 1355-1364.
[38] C. Lacroix, I. Fish, H. Torosyan, P. Parathaman, J.J. Irwin, B.K. Shoichet, S. Angers, Identification of Novel Smoothened Ligands Using Structure-Based Docking, PLoS One, 11 (2016) e0160365.
[39] S. Tian, H. Sun, P. Pan, D. Li, X. Zhen, Y. Li, T. Hou, Assessing an ensemble docking-based virtual screening strategy for kinase targets by considering protein flexibility, J. Chem. Info. Model., 54 (2014) 2664-2679.
[40] S. Tian, H. Sun, Y. Li, P. Pan, D. Li, T. Hou, Development and evaluation of an integrated virtual screening strategy by combining molecular docking and pharmacophore searching based on multiple protein structures, J. Chem. Info. Model., 53 (2013) 2743-2756.
[41] P. Cozzini, G.E. Kellogg, F. Spyrakis, D.J. Abraham, G. Costantino, A. Emerson, F. Fanelli, H. Gohlke, L.A. Kuhn, G.M. Morris, M. Orozco, T.A. Pertinhez, M. Rizzi, C.A. Sotriffer, Target flexibility: an emerging consideration in drug discovery and design, J. Med. Chem., 51 (2008) 6237-6255.
[42] C. B-Rao, J. Subramanian, S.D. Sharma, Managing protein flexibility in docking and its applications, Drug Discov. Today, 14 (2009) 394-400.
[43] X. Kong, P. Pan, D. Li, S. Tian, Y. Li, T. Hou, Importance of protein flexibility in ranking inhibitor affinities: modeling the binding mechanisms of piperidine carboxamides as Type I1/2 ALK inhibitors, Phys. Chem. Chem. Phys., 17 (2015) 6098-6113.
[44] M. Shen, S. Tian, P. Pan, H. Sun, D. Li, Y. Li, H. Zhou, C. Li, S.M.-Y. Lee, T. Hou, Discovery of Novel ROCK1 Inhibitors via Integrated Virtual Screening Strategy and Bioassays, Sci. Rep., 5 (2015) 16749.
[45] S. Zhou, Y. Li, T. Hou, Feasibility of using molecular docking-based virtual screening for searching dual target kinase inhibitors, J. Chem. Info. Model., 53 (2013) 982-996.
[46] C.A. Lipinski, F. Lombardo, B.W. Dominy, P.J. Feeney, Experimental and computational approaches to estimate solubility and permeability in drug discovery and development settings, Adv. Drug Deliv. Rev., 46 (2001) 3-26.
[47] S. Tian, J. Wang, Y. Li, D. Li, L. Xu, T. Hou, The application of in silico drug-likeness predictions in pharmaceutical research, Adv. Drug Deliv. Rev., 86 (2015) 2-10.
[48] S. Tian, J. Wang, Y. Li, X. Xu, T. Hou, Drug-likeness analysis of traditional Chinese medicines: Prediction of drug-likeness using machine learning approaches, Mol. Pharm., 9 (2012) 2875-2886.
[49] W.P. Walters, M.T. Stahl, M.A. Murcko, Virtual screening - an overview, Drug Discov. Today, 3 (1998) 160-178.
[50] T. Liu, Y. Lin, X. Wen, R.N. Jorissen, M.K. Gilson, BindingDB: a web-accessible database of experimentally determined protein-ligand binding affinities, Nucleic Acids Res., 35 (2007) D198-D201.
[51] S. Tian, X. Wang, L. Li, X. Zhang, Y. Li, F. Zhu, T. Hou, X. Zhen, Discovery of Novel and Selective Adenosine A(2A) Receptor Antagonists for Treating Parkinson's Disease through Comparative Structure-Based Virtual Screening, J. Chem. Info. Model., 57 (2017) 1474-1487.
[52] H. Sun, Y. Li, S. Tian, L. Xu, T. Hou, Assessing the performance of MM/PBSA and MM/GBSA methods. 4. Accuracies of MM/PBSA and MM/GBSA methodologies evaluated by various simulation protocols using PDBbind data set, Phys. Chem. Chem. Phys., 16 (2014) 16719-16729.
[53] H. Sun, Y. Li, M. Shen, S. Tian, L. Xu, P. Pan, Y. Guan, T. Hou, Assessing the performance of MM/PBSA and MM/GBSA methods. 5. Improved docking performance using high solute dielectric constant MM/GBSA and MM/PBSA rescoring, Phys. Chem. Chem. Phys., 16 (2014) 22035-22045.

[54] T. Hou, J. Wang, Y. Li, W. Wang, Assessing the Performance of the Molecular Mechanics/Poisson Boltzmann Surface Area and Molecular Mechanics/Generalized Born Surface Area Methods. II. The Accuracy of Ranking Poses Generated From Docking, J. Comput. Chem., 32 (2011) 866-877.

[55] C. Wang, H. Wu, V. Katritch, G.W. Han, X.-P. Huang, W. Liu, F.Y. Siu, B.L. Roth, V. Cherezov, R.C. Stevens, Structure of the human smoothened receptor bound to an antitumour agent, Nature, 497 (2013) 338-343.

[56] C. Wang, H. Wu, T. Evron, E. Vardy, G.W. Han, X.-P. Huang, S.J. Hufeisen, T.J. Mangano, D.J. Urban, V. Katritch, V. Cherezov, M.G. Caron, B.L. Roth, R.C. Stevens, Structural basis for Smoothened receptor modulation and chemoresistance to anticancer drugs, Nat. Commun., 5 (2014) 4355.

[57] U. Weierstall, D. James, C. Wang, T.A. White, D. Wang, W. Liu, J.C.H. Spence, R.B. Doak, G. Nelson, P. Fromme, R. Fromme, I. Grotjohann, C. Kupitz, N.A. Zatsepin, H. Liu, S. Basu, D. Wacker, G.W. Han, V. Katritch, S. Boutet, M. Messerschmidt, G.J. Williams, J.E. Koglin, M.M. Seibert, M. Klinker, C. Gati, R.L. Shoeman, A. Barty, H.N. Chapman, R.A. Kirian, K.R. Beyerlein, R.C. Stevens, D. Li, S.T.A. Shah, N. Howe, M. Caffrey, V. Cherezov, Lipidic cubic phase injector facilitates membrane protein serial femtosecond crystallography, Nat. Commun., 5 (2014) 3309.

[58] H.M. Berman, J. Westbrook, Z. Feng, G. Gilliland, T.N. Bhat, H. Weissig, I.N. Shindyalov, P.E. Bourne, The Protein Data Bank, Nucleic Acids Res., 28 (2000) 235-242.

[59] E.F.X. Byrne, R. Sircar, P.S. Miller, G. Hedger, G. Luchetti, S. Nachtergaele, M.D. Tully, L. Mydock-McGrane, D.F. Covey, R.P. Rambo, M.S.P. Sansom, S. Newstead, R. Rohatgi, C. Siebold, Structural basis of Smoothened regulation by its extracellular domains, Nature, 535 (2016) 517-522.

[60] X.J. Zhang, F. Zhao, Y.R. Wu, J. Yang, G.W. Han, S.W. Zhao, A. Ishchenko, L.T. Ye, X. Lin, K. Ding, V. Dharmarajan, P.R. Griffin, C. Gati, G. Nelson, M.S. Hunter, M.A. Hanson, V. Cherezov, R.C. Stevens, W.F. Tan, H.C. Tao, F. Xu, Crystal structure of a multi-domain human smoothened receptor in complex with a super stabilizing ligand, Nat. Commun., 8 (2017) 15383.

[61] J. Wang, T. Hou, X. Xu, Recent Advances in Free Energy Calculations with a Combination of Molecular Mechanics and Continuum Models, Curr. Comput. Aided Drug Des., 2 (2006) 287-306.

[62] T. Hou, R. Yu, Molecular dynamics and free energy studies on the wild-type and double mutant HIV-1 protease complexed with amprenavir and two amprenavir-related inhibitors: Mechanism for binding and drug resistance, J. Med. Chem., 50 (2007) 1177-1188.

[63] D.M. Krueger, A. Evers, Comparison of structure- and ligand-based virtual screening protocols considering hit list complementarity and enrichment factors, ChemMedChem, 5 (2010) 148-158.

[64] A. Cereto-Massague, L. Guasch, C. Valls, M. Mulero, G. Pujadas, S. Garcia-Vallve, DecoyFinder: an easy-to-use python GUI application for building target-specific decoy sets, Bioinformatics, 28 (2012) 1661-1662.

[65] V. Hornak, R. Abel, A. Okur, B. Strockbine, A. Roitberg, C. Simmerling, Comparison of multiple amber force fields and development of improved protein backbone parameters, Proteins, 65 (2006) 712-725.

[66] G.W. Bemis, M.A. Murcko, The properties of known drugs .1. Molecular frameworks, Journal of Medicinal Chemistry, 39 (1996) 2887-2893.

Legend of Figures

Figure 1. Representative smoothened antagonists in advanced development.

Figure 2. Distributions of the docking scores of VD1 for the four available Smo crystal complexes by using SP and XP scoring modes of *Glide* docking.

Figure 3. Distributions of the docking scores of VD2 for the four available Smo crystal complexes by using SP and XP scoring modes of *Glide* docking.

Figure 4. Hh signaling pathway inhibitory activity (IC_{50}) of compound **20** using NIH3T3-GRE-Luc reporter gene assay.

Figure 5. Inhibition of BODIPY-cyclopamine fluorescence signaling in the competitive displacement experiment. (a) BODIPY-cyclopamine competition with vismodegib analysis tested by fluorescent microscope at different concentrations. (b) BODIPY-cyclopamine competition with compound **20** analysis tested by fluorescent microscope at different concentrations.

Figure 6. Chemical structures of identified Smo antagonists with IC_{50} under 10 μM using docking-based virtual screening.

Figure 7. The predicted conformations and interaction patterns of (a) compound **14** in the binding pocket applying 4QIM as docking structure and (b) compound **20** in the binding pocket applying 4JKV as docking structure.

Figure 8. The correlation coefficient (r^2) between the biological activities (pIC_{50}) of 13 Smo antagonists (compound **20** and 12 analogues) and (a) the docking scores predicted using SP mode of *Glide* docking, (b) the total binding free energies predicted by the MM/GBSA based on the solute dielectric constant of 1.

Figure 9. (a) The binding pose of compound **20** derived from the MM/GBSA minimization stage (the favorable and unfavorable residues for antagonist binding are colored in blue and red, respectively), antagonist-residues interaction spectra of four representative Smo antagonists: (b) compound **20**, (c) compound **20-3**, (d) compound **20-5** and (e) compound **20-12**.

Figure 10. The detailed interaction patterns of four Smo crystal complexes. The classical and non-classical hydrogen bonds are colored in green and gray, respectively.

728 **Table1**. The docking power and discrimination power of the *Glide* docking for the
729 four Smo-antagonist crystal complexes of **VD1** and **VD2**

PDB ID	Ligand	Docking power (RMSD/Å)		Discrimination power(*P*-value)			
				VD1		**VD2**	
		SP	XP	SP	XP	SP	XP
4JKV	LY2940680	2.26	2.30	2.13×10^{-237}	1.98×10^{-128}	2.21×10^{-162}	1.16×10^{-92}
4N4W	SANT1	1.77	1.93	1.40×10^{-84}	2.16×10^{-10}	1.02×10^{-51}	5.03×10^{-24}
4O9R	Cyclopamine	4.11	0.61	4.34×10^{-57}	5.77×10^{-22}	1.72×10^{-40}	4.66×10^{-18}
4QIM	Anta XV	2.24	2.25	0	6.56×10^{-70}	5.78×10^{-123}	1.58×10^{-64}

730
731
732
733
734
735
736
737
738
739
740
741
742
743
744
745
746
747
748
749
750
751
752
753
754
755
756
757
758
759
760
761
762
763

Table 2. Biological activities, representative molecular properties and key parameters identified in docking-based VS of the 21 purchased compounds from ChemDiv database

Compd	ID_number[a]	N-G-L IC_{50} (nM) ± SEM[b]	docking score[c]	MW[d]	log*P*[e]	log*S*[f]	similarity[g]	structure[h]
1	C326-0256	>10000	-12.09	516.57	4.60	-6.28	0.34	4JKV
2	8009-2945	>10000	-11.20	485.99	5.97	-8.85	0.52	4JKV
3	5182-3585	>10000	-11.19	530.00	2.91	-7.33	0.25	4QIM
4	K400-10138	>10000	-10.55	506.64	4.64	-8.16	0.28	4QIM
5	C075-0142	>10000	-10.57	485.52	3.87	-7.42	0.26	4QIM
6	K892-0135	>10000	-11.03	492.52	4.16	-6.93	0.37	4JKV
7	F443-0633	>10000	-11.34	479.90	5.79	-7.57	0.41	4JKV
8	V023-8072	>10000	-11.16	473.58	6.05	-7.82	0.27	4JKV
9	K781-9640	>10000	-11.17	499.58	4.27	-7.23	0.50	4JKV
10	G802-0671	>10000	-10.92	447.56	4.35	-7.02	0.39	4JKV
11	G795-0588	>10000	-10.62	470.55	4.93	-6.37	0.38	4QIM
12	C241-2115	>10000	-11.01	490.58	2.86	-5.45	0.35	4QIM
13	8139-0324	>10000	-11.35	437.42	3.03	-4.32	0.37	4QIM
14	C522-1924	950 ± 450	-11.29	465.02	4.82	-7.08	0.36	4QIM
15	G435-0188	4600 ± 2800	-11.03	453.59	3.69	-6.11	0.32	4QIM
16	K784-7096	>10000	-12.00	552.09	3.22	-6.06	0.32	4QIM
17	V029-7360	2400 ± 1000	-11.43	457.48	3.88	-4.82	0.45	4JKV
18	F550-3944	3000 ± 600	-11.48	471.56	2.34	-5.07	0.29	4JKV
19	V015-8739	1200 ± 57	-11.51	451.47	4.86	-5.97	0.38	4JKV
20	C794-1677	47 ± 15	-11.82	492.69	6.08	-6.36	0.29	4JKV
21	V004-1819	>10000	-10.77	470.50	4.02	-7.20	0.34	4QIM
22	**Vismodegib**[i]	46 ± 22		421.30	4.00	-6.10		

[a]The compound number labeled in the ChemDiv database. According to the purity statements, the purity of all compounds purchased from the ChemDiv database is higher than 95%. [b]Inhibition of luminescence signaling in NIH3T3-GRE-Luc reporter gene assay (N-G-L) with 10 nM SAG as the Hh pathway agonist. Data are expressed as geometric mean values of at least two runs ± the standard error measurement (SEM).[c]The predicted binding affinity evaluated by docking score for each compound employing XP scoring function based on 4JKV or 4QIM crystal complex. [d]Molecular weight. [e]The predicted octanol/water partition coefficient. [f]The predicted aqueous solubility. [g]Pairwise similarity (*Tanimoto coefficient*) based on the FCFP_4 fingerprints for each identified antagonist with the most similar known Smo antagonist. [h]Crystal complex of Smo receptor applied in the docking-based VS. [i]Vismodegib was run as standard in each assay. Data are expressed as geometric mean values of six runs ± the standard error measurement (SEM).

783 **Table 3.** Biological activities against Smo receptor and chemical structures for the 12
784 analogues of compound **20**

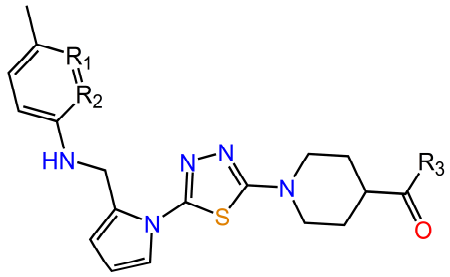

Compd	R_1	R_2	R_3	N-G-L IC_{50} (nM) ± SEM[a]	pIC_{50}	docking score[b]	ΔG_{pred}[c]
20	C	C	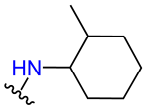	47 ± 15	7.33	-11.82	-71.28
20-1	N	C	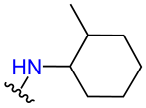	240 ± 69	6.62	-9.40	-68.95
20-2	C	N	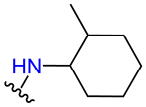	58 ± 3.4	7.24	-11.16	-71.76
20-3	C	C	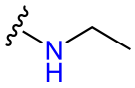	5200 ± 220	5.28	-10.48	-59.75
20-4	C	C	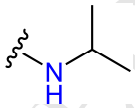	1200 ± 22	5.92	-10.62	-61.71
20-5	C	C	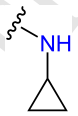	4200 ± 46	5.38	-10.51	-57.72
20-6	C	C	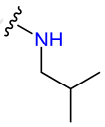	1100 ± 8.5	5.96	-10.89	-64.48
20-7	C	C	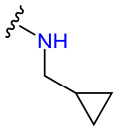	1700 ± 370	5.77	-10.78	-64.80
20-8	C	C	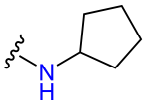	530 ± 47	6.28	-10.36	-68.57
20-9	C	C	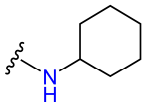	660 ± 300	6.18	-10.82	-68.15
20-10	C	C	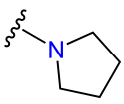	4300 ± 890	5.37	-10.05	-60.71

20-11	C	C	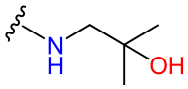	4300 ± 2200	5.37	-9.95	-65.63
20-12	C	C	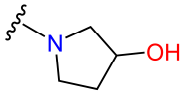	7600 ± 49	5.12	-8.95	-51.80

[a]Inhibition of luminescence signaling in NIH3T3-GRE-Luc reporter gene assay (N-G-L) with 10 nM SAG as the Hh pathway agonist. Data are expressed as geometric mean values of at least two runs ± the standard error measurement (SEM). [b]The predicted binding affinity evaluated by docking score for each compound by employing SP scoring function based on 4JKV crystal complex. [c]The predicted total binding free energies between each compound and Smo receptor (PDB ID: 4JKV, ε_{in} = 1.0)

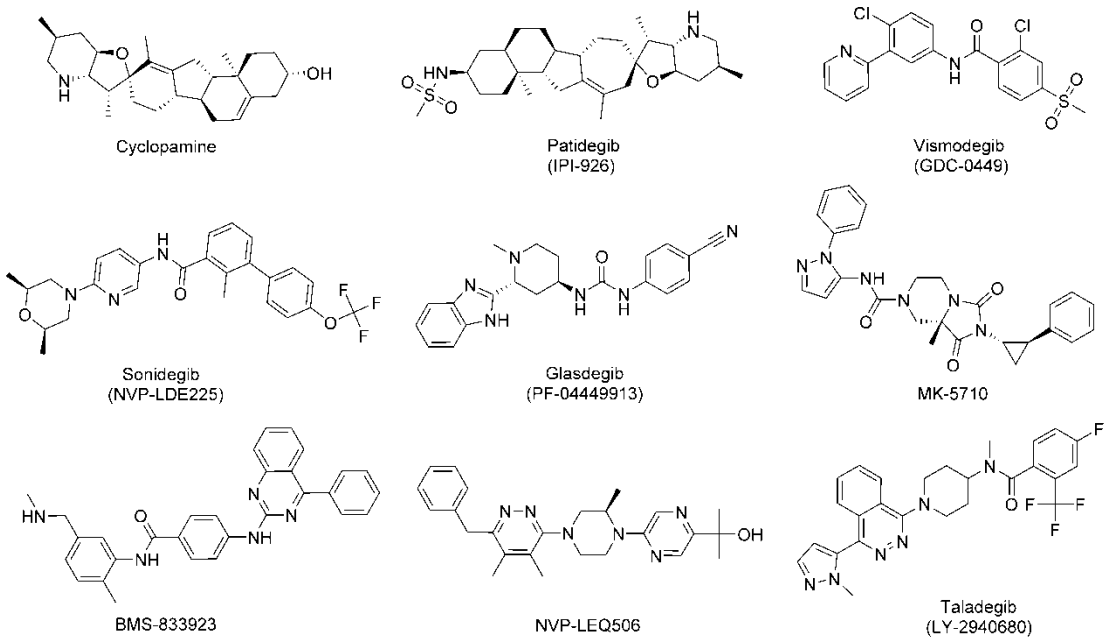

Figure 1

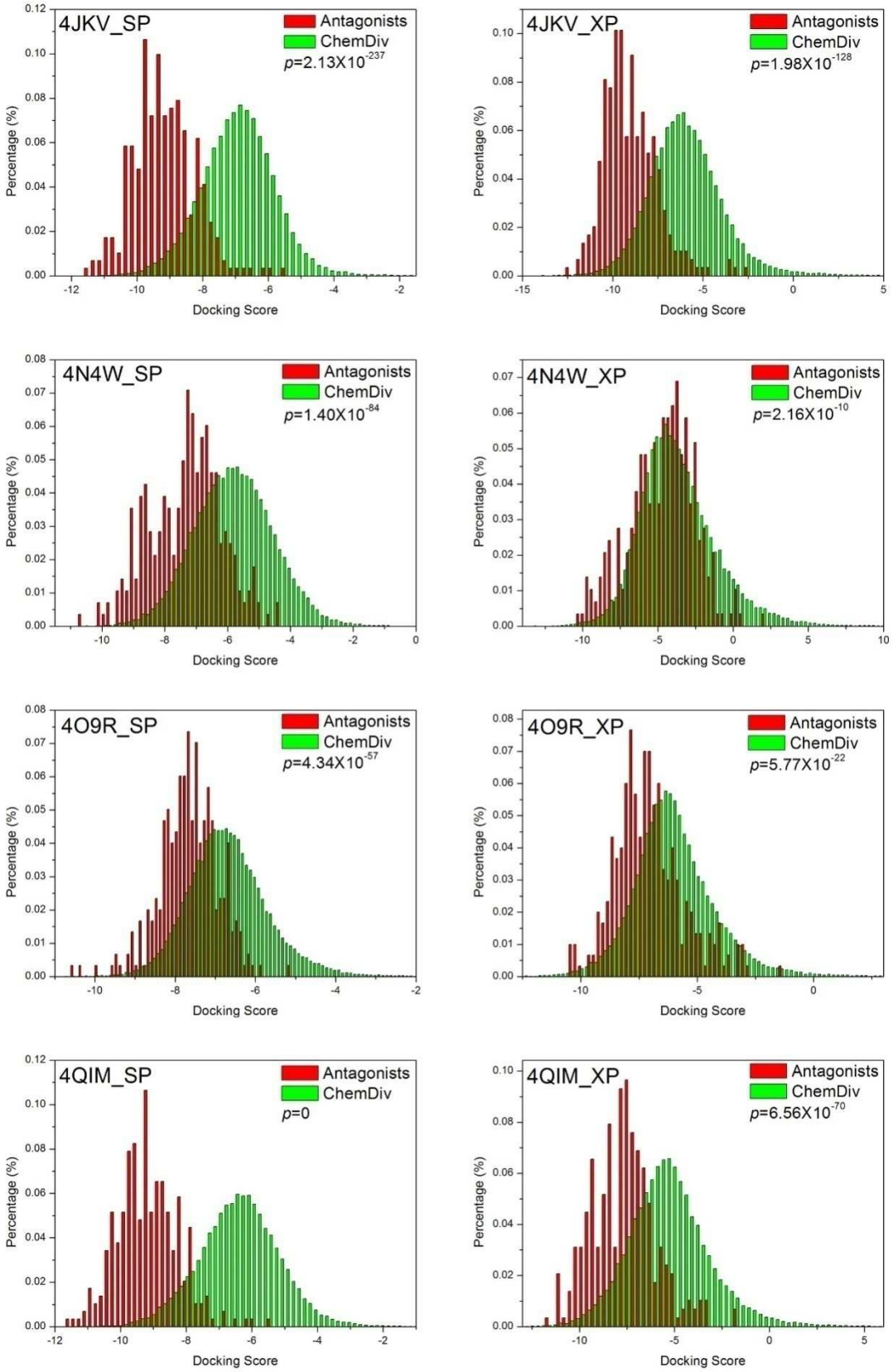
4JKV_SP
Antagonists
ChemDiv
p=2.13X10-237
4JKV_XP
Antagonists
ChemDiv
p=1.98X10-128
4N4W_SP
Antagonists
ChemDiv
p=1.40X10-84
4N4W_XP
Antagonists
ChemDiv
p=2.16X10-10
4O9R_SP
Antagonists
ChemDiv
p=4.34X10-57
4O9R_XP
Antagonists
ChemDiv
p=5.77X10-22
4QIM_SP
Antagonists
ChemDiv
p=0
4QIM_XP
Antagonists
ChemDiv
p=6.56X10-70
Percentage (%)
Docking Score

Figure 2

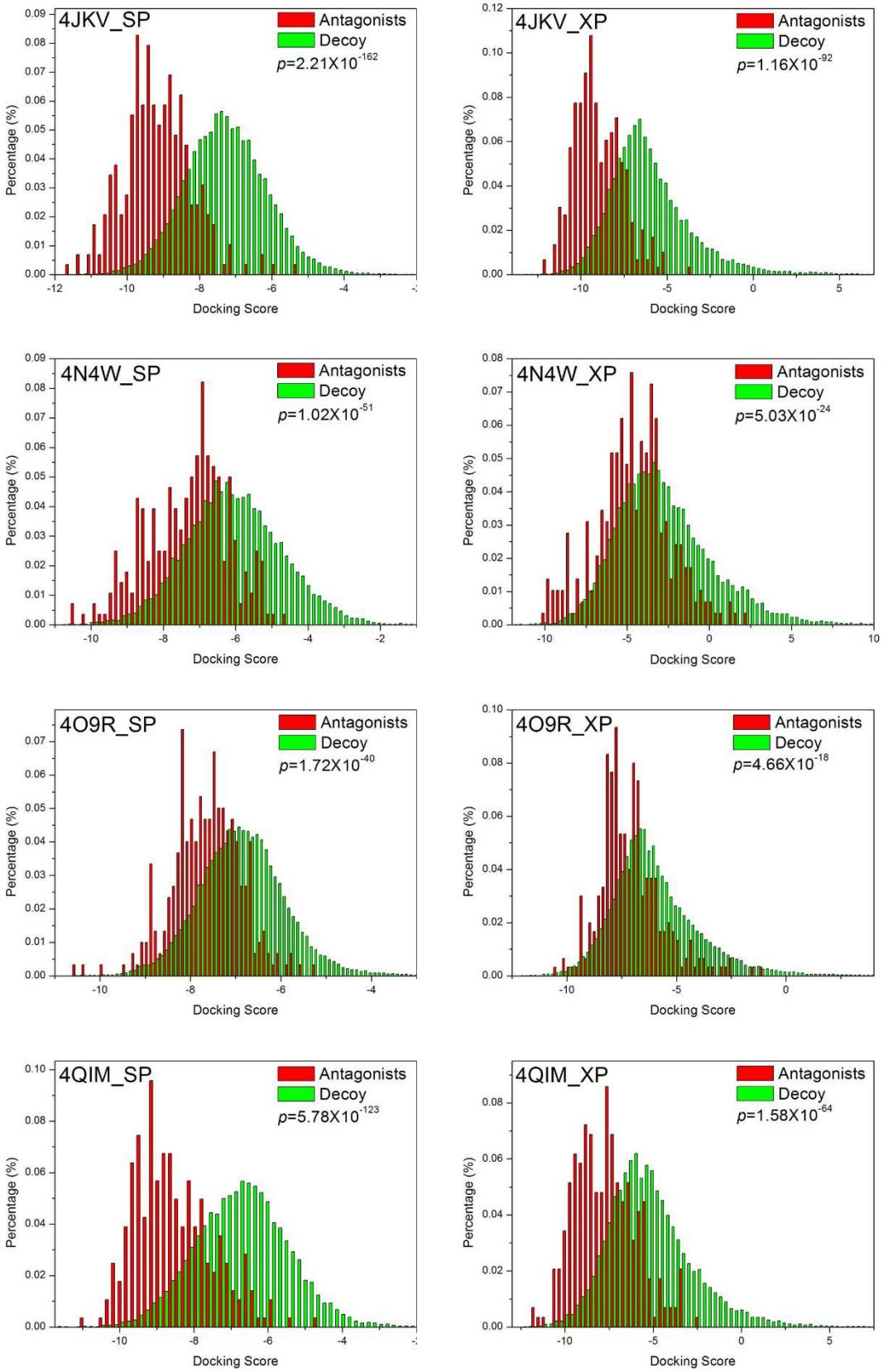
4JKV_SP
Antagonists
Decoy
p=2.21X10-162
4JKV_XP
p=1.16X10-92
4N4W_SP
p=1.02X10-51
4N4W_XP
p=5.03X10-24
4O9R_SP
p=1.72X10-40
4O9R_XP
p=4.66X10-18
4QIM_SP
p=5.78X10-123
4QIM_XP
p=1.58X10-64
Percentage (%)
Docking Score

Figure 3

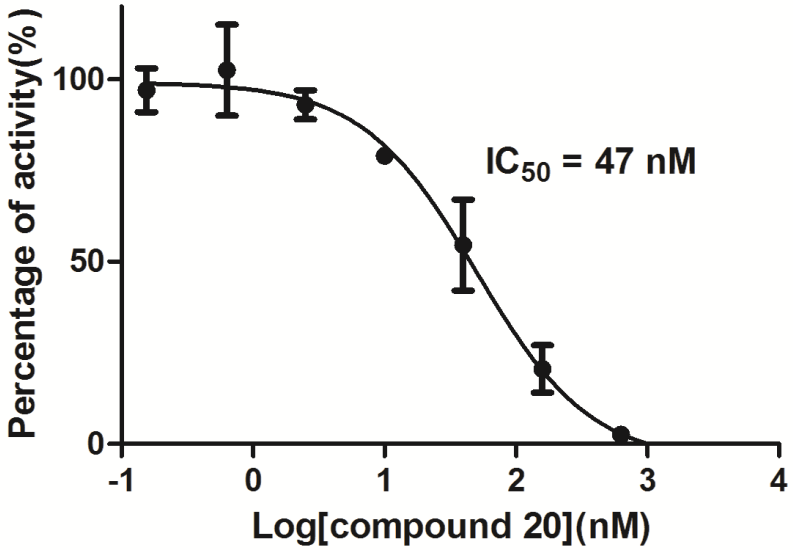

838
839 **Figure 4**
840
841
842
843
844
845
846
847
848
849
850
851
852
853
854
855

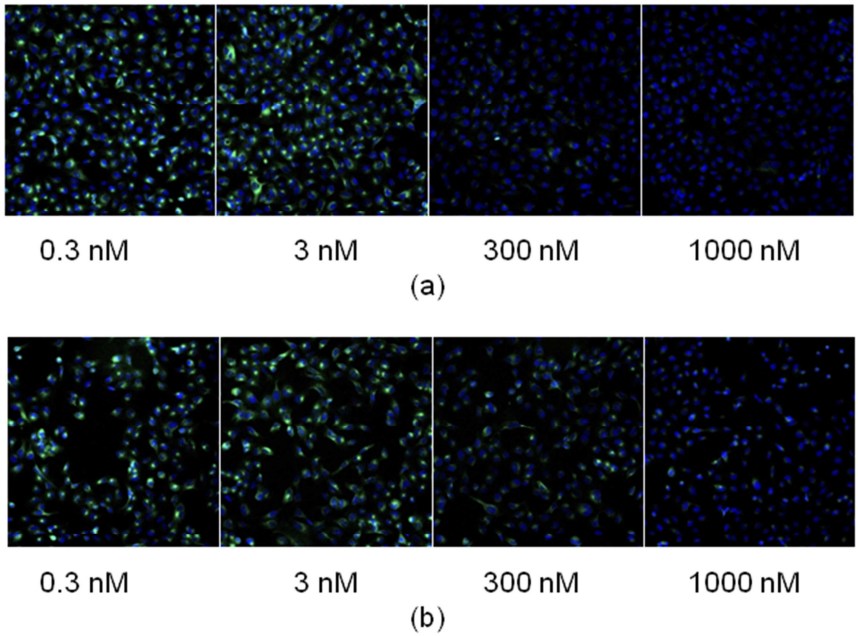

Figure 5

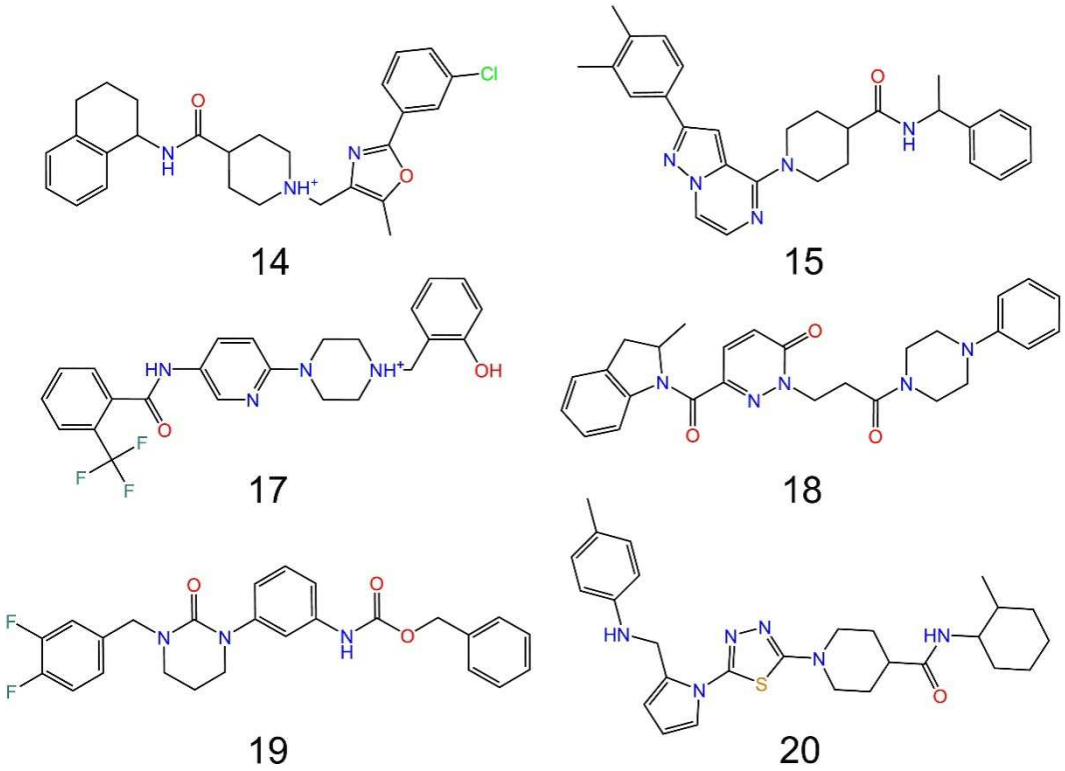

Figure 6

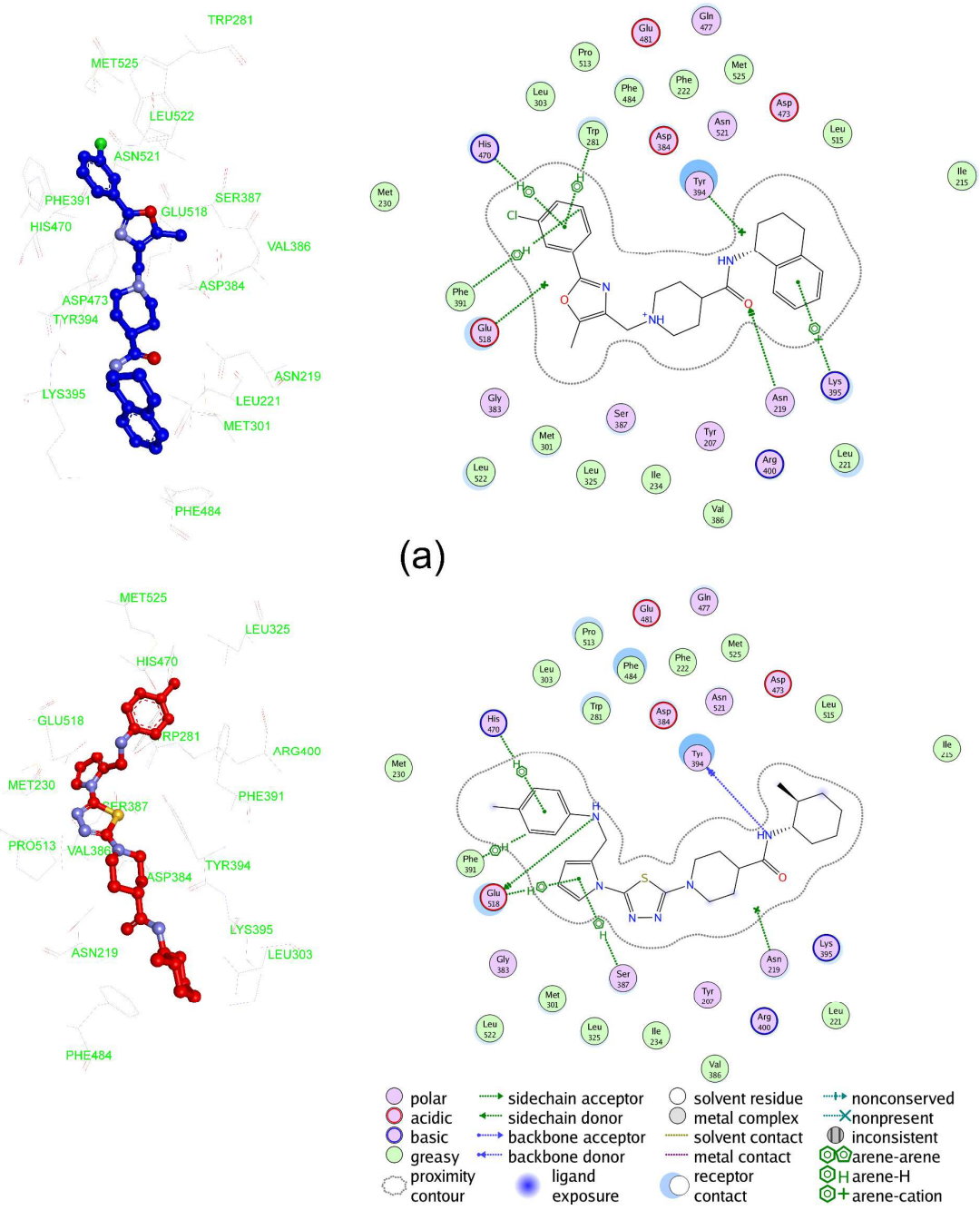
TRP281
MET525
LEU522
ASN521
PHE391
SER387
GLU518
HIS470
VAL386
ASP384
ASP473
TYR394
ASN219
LYS395
LEU221
MET301
PHE484
(a)
MET525
LEU325
HIS470
GLU518
TRP281
ARG400
MET230
PHE391
SER387
PRO513
VAL386
TYR394
ASP384
LYS395
ASN219
LEU303
PHE484
(b)
polar
acidic
basic
greasy
proximity contour
sidechain acceptor
sidechain donor
backbone acceptor
backbone donor
ligand exposure
solvent residue
metal complex
solvent contact
metal contact
receptor contact
nonconserved
nonpresent
inconsistent
arene-arene
arene-H
arene-cation

Figure 7

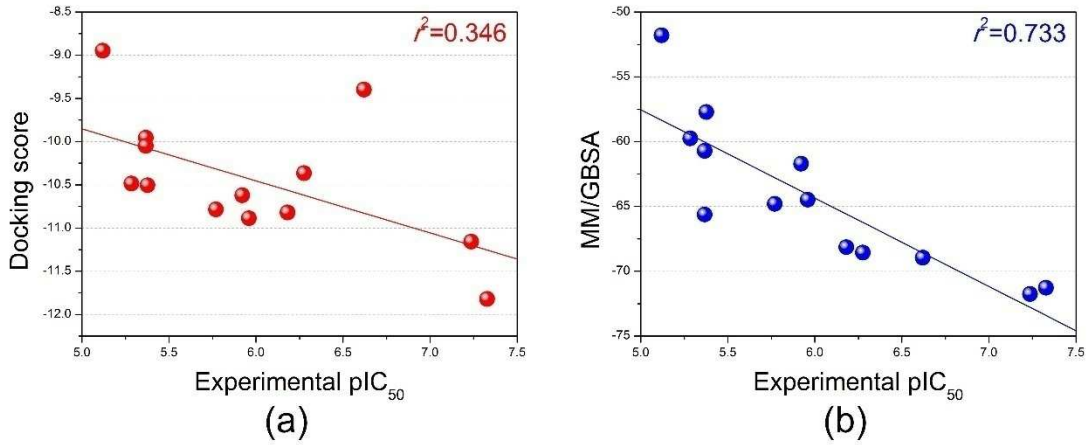

Figure 8

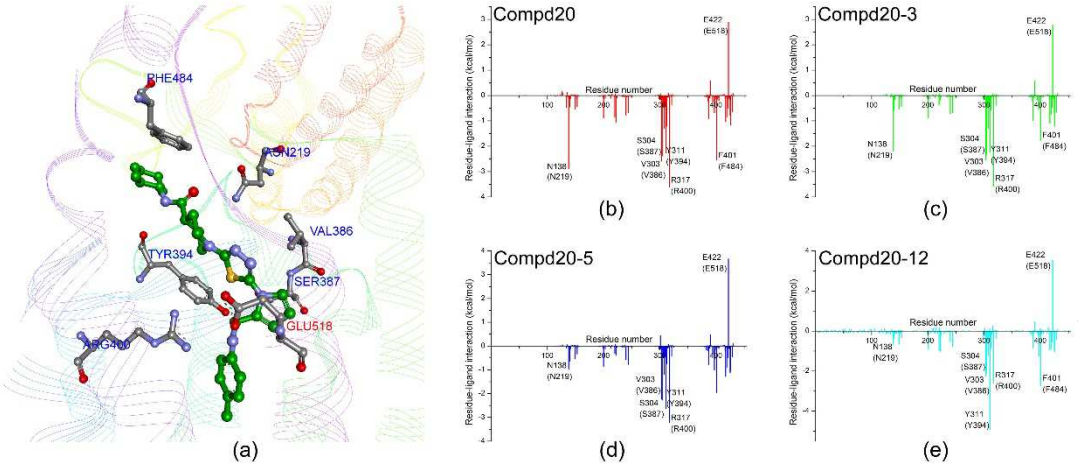

Figure 9

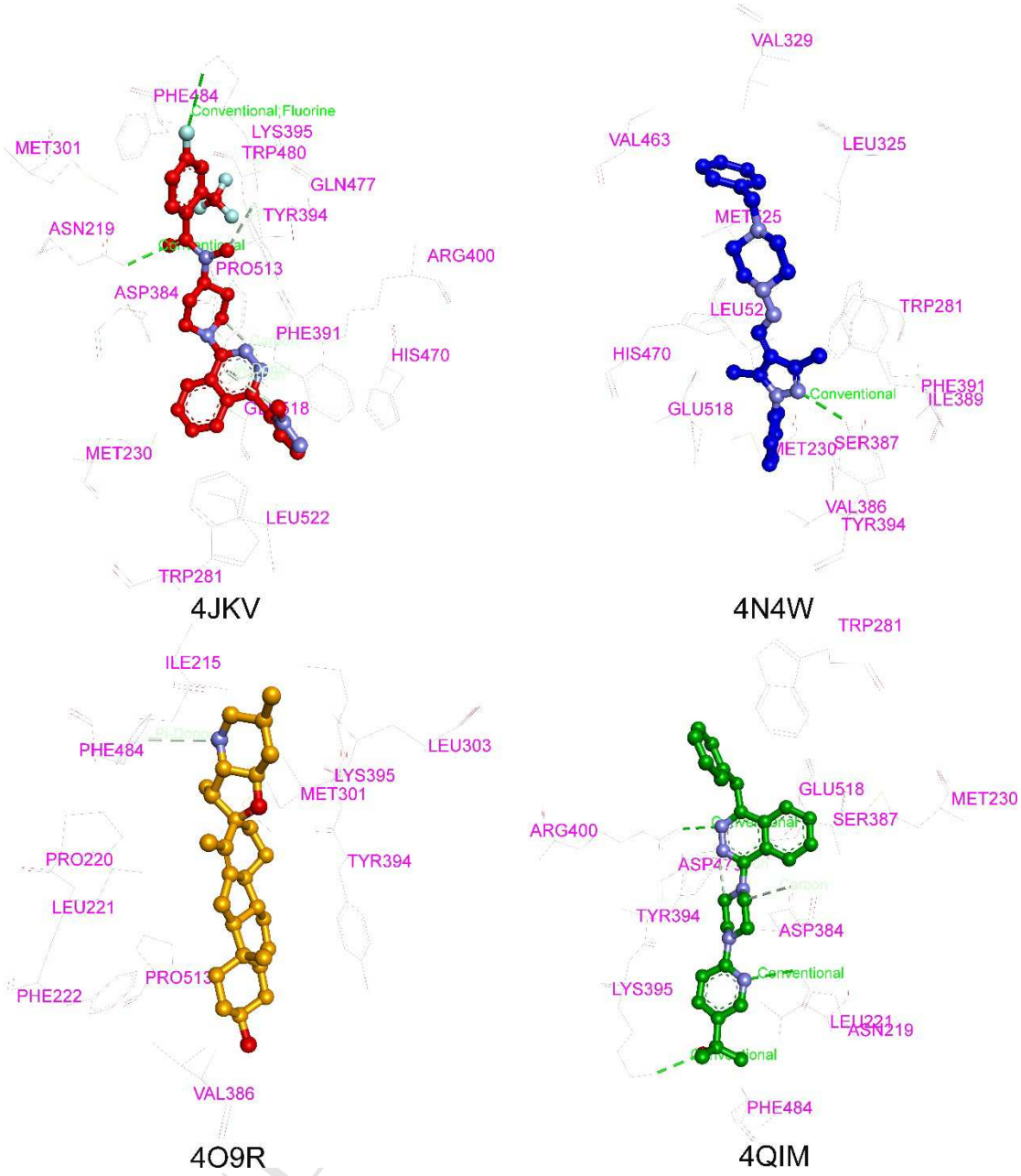
PHE484
Conventional Fluorine
LYS395
MET301
TRP480
GLN477
TYR394
ASN219
ARG400
PRO513
ASP384
PHE391
HIS470
MET230
LEU522
TRP281
4JKV
VAL329
VAL463
LEU325
TRP281
HIS470
PHE391
ILE389
Conventional
GLU518
SER387
VAL386
TYR394
4N4W
ILE215
PHE484
LEU303
LYS395
MET301
PRO220
TYR394
LEU221
PRO513
PHE222
VAL386
4O9R
TRP281
GLU518
MET230
SER387
ARG400
TYR394
ASP384
Conventional
LYS395
LEU221
ASN219
PHE484
4QIM

Figure 10

(1) A reliable docking-based virtual screening (VS) strategy for smoothened (SMO) receptor was developed.
(2) Several potent SMO antagonists with novel scaffolds were identified utilizing the VS strategy.
(3) Compound **20** (IC_{50}=47 nM) exhibited comparable hedgehog signaling inhibition to vismodegib (46 nM).
(4) The SAR and predicted binding patterns for these potent Smo antagonists were analyzed.